Techno-economic modeling framework to assess the feasibility of hydrogen-powered trains on non-electrified routes

Journal of Power Sources 652 (2025) 237677

Contents lists available at ScienceDirect

Journal of Power Sources

journal homepage: www.elsevier.com/locate/jpowsour

Techno-economic modeling framework to assess the feasibility of hydrogen-powered trains on non-electrified routes

Gabriele Peyrani [a,*], Paolo Marocco [a], Marta Gandiglio [a], Pierpaolo Cherchi [b], Massimo Santarelli [a]

[a] Department of Energy, Politecnico di Torino, Corso Duca degli Abruzzi 24, 10129, Torino, Italy
[b] Alstom Ferroviaria S.p.a., Via O. Moreno, 23, 12038, Savigliano (CN), Italy

HIGHLIGHTS

- Hydrogen enables decarbonization of long, non-electrified railways with tough terrain.
- Comprehensive TCO analysis compares hydrogen, diesel, and electric train options.
- HMU trains cut energy use and emissions by integrating fuel cells and batteries.
- HMU competitiveness improves as diesel prices rise and hydrogen costs decline.

GRAPHICAL ABSTRACT

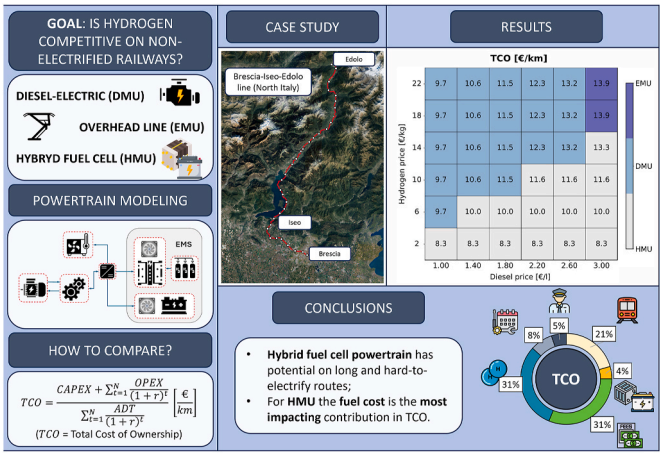

ARTICLE INFO

Keywords:
Hydrogen
Fuel cells
Batteries
Railways
Decarbonization
Cost analysis

ABSTRACT

The global transportation sector is under pressure to reduce its environmental impact, particularly greenhouse gas emissions. Rail transport is exploring innovative technologies to improve sustainability and reduce local pollution. This paper investigates the integration of fuel cell and battery technologies in hybrid fuel cell trains as a solution to decarbonize non-electrified routes. A model is developed to estimate hydrogen consumption, essential for operational planning and efficiency evaluation, alongside other key performance indicators. A Total Cost of Ownership (TCO, €/km) analysis is carried out to assess the economic viability compared to conventional diesel and electric trains. Additionally, an optimization approach is implemented to design the fuel cell and the battery sizes, with the goal of minimizing the TCO. The model is applied to a 103 km railway in northern Italy – the Brescia-Iseo-Edolo line – currently operating diesel trains, with plans to adopt fuel cell technology. Results show a hydrogen consumption of about 0.38 kg/km under beginning-of-life conditions, reducing fuel use by 46 % compared to diesel. Although the TCO of the hybrid fuel cell trains is currently higher than diesel multiple unit

* Corresponding author.
E-mail address: gabriele.peyrani@polito.it (G. Peyrani).

https://doi.org/10.1016/j.jpowsour.2025.237677
Received 16 April 2025; Received in revised form 11 June 2025; Accepted 13 June 2025
Available online 18 June 2025

trains (+6 %), the analysis confirms the potential of hydrogen for regional rail where line electrification is not economically viable.

1. Introduction

The global transportation sector is undergoing a significant transformation, driven by the urgent need to reduce greenhouse gas emissions and combat climate change. Among the various segments of this sector, rail transport shows significant promise for decarbonization, even though road transport currently garners more attention in the literature. The decarbonization potential is particularly relevant for railway lines that rely on diesel-powered trains, which are significant contributors to local air pollution and carbon emissions. This potential could further expand by increasing the transport of goods and people via railway, contributing to the decarbonization of the transport sector. Consequently, the development of new railway lines could also be considered.

Currently, the European network has a share of electrified lines amounting to nearly 57 % [1]. The two primary alternatives to diesel trains are battery-electric trains and electrification via pantographs. Battery-electric trains are promising in efficiency terms, but they encounter significant limitations related to weight and volume when driving range grows, making them less feasible for routes longer than 80 km [2]. On the other hand, electrification through overhead lines and connection through pantographs is a well-established and mature technology that offers continuous power supply. However, the costs associated with this solution could not be worth it in cases where numerous obstacles are present (e.g., tunnels and bridges), as they can drive specific installation costs to the order of M€/km [3]. In this sense, the line may present infrastructural challenges that make the installation of overhead lines more expensive and even impractical.

One innovative solution that is gaining attention for non-electrified lines is the integration of fuel cell (FC) and battery technologies in the Hydrogen Multiple Unit (HMU) train. These trains offer a potential pathway to sustainable rail transport by combining the high efficiency conversion of fuel cells compared with diesel engines, with the quick-response energy storage behavior of batteries. They can leverage the benefits of hydrogen fuel cells both as prime movers and especially as range extenders for long-range travel, while batteries enable energy-efficient operation, rapid responsiveness and permit energy recovery during braking phases. This combination provides a balanced solution to the challenges of weight, range, costs, and infrastructural limitations.

The effective operation of such hybrid hydrogen-battery configurations requires dedicated energy management strategies (EMS) to coordinate power flows and ensure efficiency, responsiveness, and component durability. Regarding some simple but effective EMS applied in railway sector, the Equivalent Consumption Minimization Strategy (ECMS) is widely used. Fragiacomo et al. [4] exploited a hybrid strategy composed of ECMS and fuzzy logic control to take advantage of the features of their modeled powertrain (fuel cell-battery-supercapacitor). Other studies have employed simpler methods, such as Rule Based (RB) approaches, which rely on if/then logics. For instance, Jiang et al. [5] utilized a rule-based controller to manage the power splitting of the hybrid fuel cell-battery powertrain, using only the State of Charge (*SoC*) and power demand as inputs. Kapetanović et al. [6] provided a comprehensive analysis of fuel consumption in hydrogen fuel cell trains, while experimental validation was also included in the work by Akhoundzadeh et al. [7]. Others gave importance to fault diagnosis of PEMFC with advanced methods [8], which could improve the economic competitiveness of this technology by reducing maintenance costs. Other works [9,10] have explored more advanced and precise EMS, such as Model Predictive Control (MPC), which optimizes the power management at each time instant, but inevitably increases the computational cost and the number of input parameters.

However, none of the aforementioned studies offer a methodology to assess the economic impact of the HMU technology compared to commercial alternatives. Other works presented a complete overview of the economic implications of HMU deployment, with different case studies and train types, but without addressing a detailed energy consumption modeling. Zenith et al. [11] made a comprehensive analysis of the usage of different innovative propulsion systems for freight movement. Their results indicate the potential of fuel cells and batteries to replace diesel on rail lines with low traffic volumes, where electrification may not be convenient. However, the propulsion system of each type of train was not modeled, but constant energy conversion efficiencies were considered. One of the major contributions comes from Roland Berger's report [12], which analyzed an ideal case study constituted by a flat 100-km route with 10 stops, revealing that the HMU has a Total Cost of Ownership (TCO, in €/km) slightly higher than a Diesel Multiple Unit (DMU). In particular, regional passenger trains are the type of railway transport that has the smallest cost increase compared to the conventional DMU case (+6 % of the TCO), while for shunters and mainline locomotives the increase is larger (13–14 %). This outcome further suggests that regional passenger transport could be the most suitable application for HMU technology.

1.1. Aims and novelty of the study

This work presents several novel contributions in the field of hydrogen-powered rail transport and comparative techno-economic modeling of train propulsion systems. Its main objective is to develop a modeling framework that integrates both technical and economic aspects. The key contributions of this study are outlined below.

- Multi-technology assessment: the study compares three propulsion technologies – Hydrogen Multiple Unit (HMU), Diesel Multiple Unit (DMU), and Electric Multiple Unit (EMU) – applied to a non-electrified line, considering all the route and vehicle characteristics that can affect energy consumption (e.g., speed limits along the route, slopes, train's weight, powertrain's dynamic efficiency behavior, etc.). Additionally, the analysis includes economic performance under variable energy cost scenarios (e.g. hydrogen and diesel prices), offering insights into which technology is the best for the desired route depending on the context of the case study. Additionally, the robustness of the results is enhanced by validating the HMU model with data from the train manufacturer.
- Powertrain component sizing through hybridization ratio analysis: a parametric optimization approach is employed to determine the optimal sizing of fuel cell and battery components based on the hybridization ratio. This method enables the minimization of the TCO parameter, balancing both capital and operational expenditures.
- Application to a real case study: the methodology is applied to the Brescia-Iseo-Edolo railway line [13], a real non-electrified Italian route where HMU deployment is already planned as part of the innovative project (H2HiseO) aimed at decarbonizing a significant portion of local public transport [14]. This increases the policy relevance of the study.
- Flexible and transferable modeling framework: the proposed simulation and cost analysis framework is modular and adaptable, enabling its application to other railway lines and propulsion configurations. The presented model offers an effective solution for guiding decarbonization strategies and decisions in the rail transport sector.

The paper is structured as follows: Sections 2.1 and 2.2 outline a

simple yet effective method to calculate the minimum time's driving cycle to complete the route and the associated hydrogen consumption. A TCO analysis is then presented in Section 2.3 to determine the economic response of the investment and to identify the most impactful costs of the project. Section 3 focuses on the propulsion system breakdown and aims to show how the powertrains work and to explain the energy management strategy. In Section 5 the results are shown, also including an in-depth analysis to determine the optimal sizes of the components in Section 5.1. Finally, section 6 summarizes the conclusions of the study.

2. Methodology

Section 2.1 develops a method to calculate the traction power of the train based on the vehicle parameters and the route characteristics (slopes, lengths, maximum velocities). In Section 2.2, a detailed analysis of the powertrain modeling is assessed and the corresponding equations to calculate the hydrogen consumption – knowing the powertrain efficiencies and parameters – are shown. Then, Section 2.3 explains the assumptions made to evaluate the TCO of the route. The structure of the proposed techno-economic modeling framework is summarized in Fig. 1, which illustrates the organization of the methodology – including the different sections highlighted by blue rectangles – as well as the main inputs and outputs.

2.1. Train and route dynamics

The first step is to determine the tractive energy needs of the train. Then the technical data regarding energy consumption will be used to calculate the economic performance.

2.1.1. Lomonossoff's equation

The motion of a train along a route can be modeled through the Lomonossoff's Equation [15], which states that by applying the Newton's law to the train's wheel, a simple equation that models all forms of transport can be obtained:

$$M' \cdot \frac{d^2x}{dt^2} = F_t(v) - \left(c \cdot \left(\frac{dx}{dt}\right)^2 + b \cdot \left(\frac{dx}{dt}\right) + e \right) - M' \cdot g \cdot \sin(\alpha) \quad (1)$$

where M' (kg) is the mass of the train M (kg) increased by the rotary allowance λ (which is dimensionless):

$$M' = M \cdot (1 + \lambda) \quad (2)$$

The term x (m) is the position at the instant t (s), while F_t (N) is the tractive force experienced by the wheel. This force depends on the velocity of the train when acceleration or deceleration is needed, following the behavior of the traction force curve, which typically has an initial plateau before decreasing hyperbolically with increasing velocity. The term g is the gravitational acceleration and α is the slope of the track. The coefficients c, b and e are the train David's coefficients, which account for the losses due to static, rolling and aerodynamic resistance, respectively. An additional term, $\frac{D}{r}$, could be included in the losses calculation to consider the curvature resistance if the data is available [16], where D (N · m) is an empirical constant and r (m) is the curve radius. However, this factor is not considered in the current study, as it is only relevant for tight curves. The velocity v (m/s) and the acceleration a (m/s^2) can be calculated as $v = \frac{dx}{dt}$ and $a = \frac{d^2x}{dt^2}$. The input parameters of the train required by Equation (1) are shown in Table 1.

2.1.2. Simulation of route dynamics

The simulation takes advantage of the Euler method to solve the differential equation in time in discrete steps. The time step width needs to be defined to have the right compromise between accuracy and computational cost. The simulation needs an initial value of the physical parameters computed during the trip at the inlet node, in order to calculate the quantities at each time step for the outlet node, assuming

Table 1
Train technical characteristics.

Characteristics	Value	Ref.
Maximum weight [t]	216	[17]
Maximum acceleration-deceleration [m/s^2]	± 0.8	Assumption
Maximum traction power [kW]	1170	[17]
Train autonomy [km]	600	[17]
Total seats [–]	260	[17]
Static resistance e [N]	CONFIDENTIAL	
Rolling resistance b [N/(km/h)]	CONFIDENTIAL	
Aerodynamic resistance c [N/(km/h)^2]	CONFIDENTIAL	
Rotary allowance λ [%]	7.0	Assumption

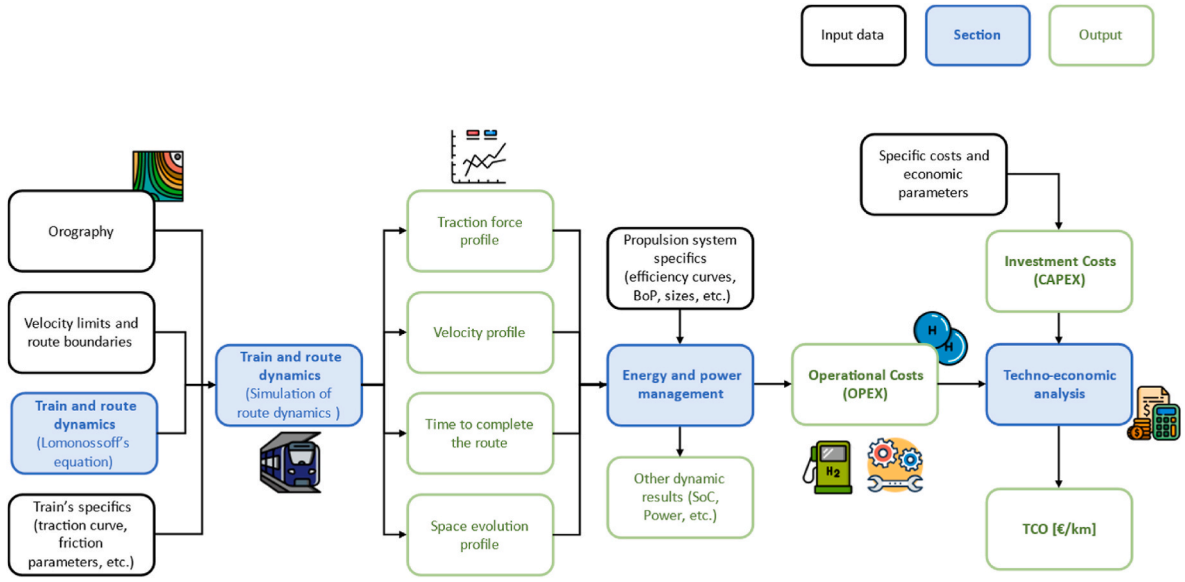

Fig. 1. Workflow of the techno-economic model for evaluating the TCO of the train propulsion system, from dynamic simulation to costs calculation. Colors indicate: black for input data, blue for sections of the manuscript, green for model outputs. (For interpretation of the references to colour in this figure legend, the reader is referred to the Web version of this article.)

them as constant between the two points. The outcomes of the solution are the velocity, acceleration, force and so the traction power, found as the product of traction force and velocity. The velocity is kept below the maximum speed limit (v_{lim}, in m/s) – provided as an input – and the acceleration presents a maximum threshold for passengers' comfort, in this case set equal to $a_{lim} = \pm\ 0.8\ \frac{m}{s^2}$. The current strategy to solve the motion equation to determine the mission profile that minimizes the time required to travel the route.

The train's operational modes can be classified into three main groups.

- **Acceleration**: As shown in the set of Equation (3), the acceleration phase solves the equation between two nodes knowing the force applied to the wheel F_t (N), the external resistive force R (N), and the gravitational force F_g (N). The latter can be either positive – if the train is climbing – or negative – if the train is descending. The acceleration a is found by dividing the resulting force F by the total mass M' and is positive. Then the velocity v_i can be computed by summing the inlet node velocity v_{i-1} and the product between the acceleration and the time step dt. The last equation shows the exit condition of the simulation ($s_i = s_{max}$), indicating that the train has to undergo a change in the motion, and it is found by intersecting the forward Euler simulation with the backward one. The term s_i (m) is the position of the train in time and s_{max} (m) is the position of the exit condition.

$$\begin{cases} F_i = F_{t,i}(v_{i-1}) - F_{g,i}(x) - R_i(v_{i-1}) \\ R_i = c{\cdot}v_{i-1}^2 + b{\cdot}v_{i-1} + e \\ 0 < a_i = \dfrac{F_i}{M'} \le a_{lim} \\ v_i = v_{i-1} + a_i{\cdot}dt \le v_{lim,i} \\ s_i = s_{i-1} + v_i{\cdot}dt + \dfrac{1}{2}a_i{\cdot}dt^2 \le s_{max} \end{cases} \tag{3}$$

- **Cruise**: Once the maximum possible velocity is reached, the train enters in the cruising phase where the only tractive effort made is to counterbalance the resistive and gravitational forces, and so the resulting acceleration is null (set of Equation (4)). Even in this phase, if the slope tends to make the train accelerate, the resulting traction force will be negative, and so a braking effort will be seen by the wheel.

$$\begin{cases} F_i = F_{t,i}(v_{i-1}) - F_{g,i}(x) - R_i(v_{i-1}) = 0 \\ R_i = c{\cdot}v_{i-1}^2 + b{\cdot}v_{i-1} + e \\ a_i = 0 \\ v_i = v_{i-1} = v_{cruise} \\ s_i = s_{i-1} + v_i{\cdot}dt \le s_{max} \end{cases} \tag{4}$$

- **Braking**: Whether the train is reaching the station or there is a decrease in the maximum speed limit, the train enters the braking mode, and so the resulting acceleration is negative. The equations that regulate this phase are represented in the set of Equation (5) and are similar to the acceleration phase, but the contributions of the gravitational and resistive forces act in the opposite direction. Indeed, if there is a downhill section in the proximity of the station, it will affect the braking phase by making the train start braking in advance. Contrariwise, if there is an uphill section, the train will start to brake overdue, since the slope will help the deceleration. Instead, resistive forces will always push the train to stop in advance.

$$\begin{cases} F_i = -F_{t,i}(v_{i-1}) - F_{g,i}(x) - R_i(v_{i-1}) \\ R_i = c{\cdot}v_{i-1}^2 + b{\cdot}v_{i-1} + e \\ -a_{lim} \le a_i = \dfrac{F_i}{M'} < 0 \\ v_i = v_{i-1} + a_i{\cdot}dt \\ s_i = s_{i-1} + v_i{\cdot}dt + \dfrac{1}{2}a_i{\cdot}dt^2 \le s_{max} \end{cases} \tag{5}$$

The set of equations is resolved for the entire round-trip with both forward and backward Euler methods with a consecutive superposition of the results. The computation needs to be held until the exit conditions on the maximum velocity ($v_i > v_{lim}$) or – as in the present case – the space between one station and the subsequent ($s_i > s_{max}$) are satisfied.

The resulting traction and braking force diagram can be seen in Fig. 2. The tractive-effort curve shows the relationship between the force a vehicle's wheels apply to the rail and its speed. It highlights how the force is highest at low speeds for acceleration and decreases as speed increases. The negative part of the graph shows the behavior of the train when the braking phase is needed and typically it is not symmetrical with the positive side of the axis.

2.2. Energy and power management

Once the laws governing the train for the selected route are known, it is possible to calculate the traction power required from the propulsion system and the related fuel consumption.

Three propulsion systems are considered and compared.

- Hydrogen Multiple Unit: the most innovative solution and the main focus of this analysis. The HMU uses a hybrid battery and fuel cell propulsion system, operated according to the strategy described in Section 2.2.2. This control strategy defines the power demand from the propulsion system, enabling the calculation of fuel consumption. Input data for this scenario is detailed in Section 3.1.
- Diesel Multiple Unit: the current propulsion system used in the case study. The train is modeled using the real efficiency curve of a railway diesel train (as shown in Section 3.2) to evaluate fuel consumption for the selected route.
- Electric Multiple Unit: a well-developed decarbonization option, modeled with the input data shown Section 3.3.

The Battery Multiple Unit (BMU) has not been considered in this

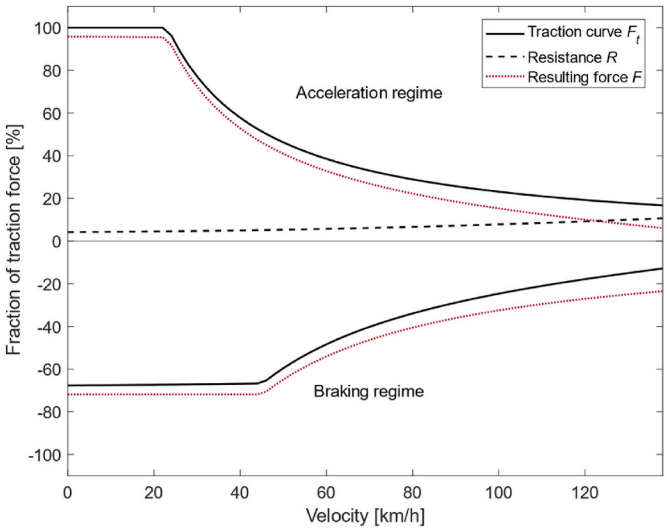

Fig. 2. Train's tractive-effort curve with 5 ‰ slope divided into acceleration and braking regimes.

analysis because, in order to achieve the same level of autonomy as the other alternatives for the selected case study, the required battery system would exceed the maximum allowable weight for the train.

The energy management strategy implemented in this study operates under the assumption of a perfectly forecasted power demand along the mission profile. While this represents a simplification, it is a reasonable assumption for offline simulations aimed primarily at system sizing, component optimization, and techno-economic assessment. Several parameters influencing power demand, such as train mass (which may vary due to passenger load), ambient temperature (affecting auxiliary loads like HVAC systems), and resistive forces (rolling and aerodynamic drag), are treated as constant in the present model. The baseline values adopted for these variables reflect realistic operational conditions, and have been validated through direct feedback from industrial stakeholders, ensuring robustness and applicability of the model. However, they are not dynamically adjusted during the mission, and their potential variability is not captured. Moreover, the current framework does not account for uncertainties related to schedule adherence (e.g., unplanned stops, delays) which can have an impact on the actual power profile and energy demand. The consideration of such stochastic elements would require a different class of models and so other kind of EMS [18], which is outside the scope of this study but represent promising directions for future work.

For the propulsion systems involved in this study, the traction power is assessed (Section 2.2.1) and fuel consumption is evaluated (Section 2.2.3). Finally, economic performance is calculated as outlined in Section 2.3.

2.2.1. Traction power

For each train operating condition (acceleration, cruise, braking), the power required by the train motion (P_t, in kW) can be computed. This power is determined as the product of the effort made on the wheel – following the tractive effort curve (force-velocity curve) – and the velocity of the train. It has to be always equal to or lower than the maximum traction power that the train can provide (P_{MAX}, in kW), as shown in Equation (6).

$$-P_{MAX} \leq P(t) = F_t(t) \cdot v(t) \leq P_{MAX} \tag{6}$$

This quantity can be either positive or negative: a positive effort on the wheel means an acceleration of the train, while a negative one would mean that the brakes are in operation. When the train brakes, the braking system allows for the recovery of part of the braking energy, which is stored in an electrochemical storage system. The DMU and EMU do not have batteries and so no strategy and regenerative braking will be considered.

2.2.2. Energy system strategy for HMU

The HMU's powertrain is fully electric, consisting of a hydrogen-powered Proton Exchange Membrane Fuel Cell (PEMFC) and a battery system. The presence of the battery makes the HMU a hybrid propulsion system. This configuration allows the battery to assist the fuel cell in satisfying the steepest load changes throughout the route, thereby reducing the FC aging and meeting the power requests that exceed the FC capacity.

Furthermore, the energy management system should enable power to be supplied by both the fuel cell and the battery in a smart and efficient way. The energy management system allows for calculating the power delivered by the FC and the battery throughout the mission according to the following criteria.

- Charge sustaining mode: the aim is to maintain a null variation in the battery's State of Charge (SoC) after a complete cycle (round trip), while keeping the SoC within the range of 20 % (SoC_{min}) and 80 % (SoC_{max}) to preserve battery performance and avoid the need for expensive fast charging infrastructures at the stations [19]. The SoC indicates the charge level relative to the total capacity (BAT_{cap}, in kWh). This assumption was made to ensure a fair comparison between the different propulsion systems and to evaluate the train's energy consumption only in terms of hydrogen consumed.
- The FC should assist in recharging the batteries together with the energy coming from the braking system in order to follow the reference state of charge (SoC_{ref}).
- The FC should be able to modulate power requests from the total net electric load at the exit of the converter (P_{load}, in kW), the Balance of Plant (BoP) of the system (P_{BoP}, in kW) and the passengers' comfort request (P_{aux}, in kW). FC maximum current ramp-up ($\left(\frac{dI}{dt}\right)_{max}$, in A/s) and ramp-down rates ($\left(\frac{dI}{dt}\right)_{min}$, in A/s) are imposed in order to slow the aging of the component. Additionally, to remain within the limits of the installed FC capacity, a maximum net power output equal to its size (FC_{size}, in kW) has been set. The interaction between these parameters can be found in Equations (9) and (10).

In order to match all the previous constraints and to exempt the FC from a simple load following, an Equivalent Consumption Minimization Strategy (ECMS) has been applied [20].

The interactions described in the following equations are summarized and visually clarified in the schematic diagram shown in Fig. 3, which highlights the main power flows of the hybrid propulsion system. As shown in Equation (7), P_{load} can be calculated considering the power demand and the efficiencies involved, divided in the case of positive and negative effort:

$$P_{load}(t) = \begin{cases} \dfrac{P_t(t)}{\eta_{gear} \cdot \eta_{motor}}, \text{if } P_t(t) \geq 0 \\ P_{brk}(t) \cdot \eta_{gear} \cdot \eta_{motor}, \text{if } P_t(t) < 0 \end{cases} \tag{7}$$

P_{brk} (kW) is the regenerative power recovered during braking, which is multiplied by the regenerative braking efficiency, equal to the product of the two efficiencies η_{gear} and η_{motor} which represent the gears and electric motors, respectively [21].

Regarding the management strategy, the ECMS introduces an equivalence factor j, which is applied during the mission to the power delivered by the FC. The purpose is to encourage the battery to keep the desired state of charge (SoC_{ref}). The equivalence factor formulation is shown in Equation (8):

$$j(t) = \left[1 - k_p \cdot \left(\frac{SoC(t) - \frac{SoC_{max}+SoC_{min}}{2}}{\frac{SoC_{max}-SoC_{min}}{2}}\right)^n\right] \cdot \left[k_a \cdot \left(SoC_{ref} - SoC(t)\right) + \frac{j(t-1)+j(t-2)}{2}\right] \tag{8}$$

where k_p, k_a and n are the parameters used to tune the strategy, $j(t-1)$ and $j(t-2)$ are the equivalence factors at the previous steps. The tuning of the parameters k_p, k_a and n has been made through the NSGA (Non-Dominated Sorting Genetic Algorithm) optimization tool with the

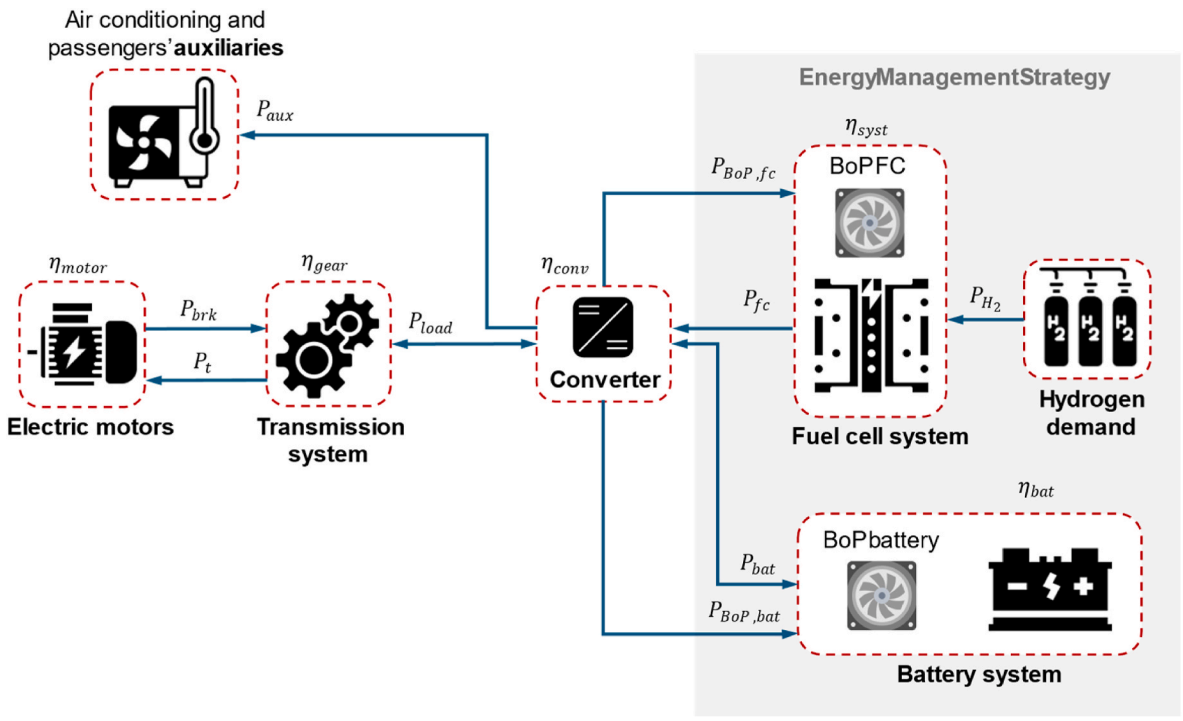

Fig. 3. Hydrogen Multiple Unit propulsion system breakdown.

following objective functions to be minimized:

- ΔSoC: the difference between the *SoC* at the end of the trip and the reference value should be minimized or even put equal to zero.
- Hydrogen consumption: parameter tuning also targets a reduction in total hydrogen usage over the mission.
- *SoC* penalty: a penalty is introduced when the *SoC* exceeds the predefined maximum threshold (SoC_{max}) or drops below the minimum threshold (SoC_{min}).

The FC behavior can be modeled as in Equations (9) and (10). It explains the constraints applied to the FC power P_{fc} (kW) and current I_{fc} (A) during the mission.

$$\begin{cases} P_{fc}(t) = \left(\dfrac{P_{load}(t) + P_{aux}(t) + P_{BoP}(t)}{\eta_{conv}}\right) \cdot j(t) \\ 0 \le P_{fc}(t) \le FC_{size} \end{cases} \tag{9}$$

In Equation (9), P_{BoP} is the sum of two contributions: the FC BoP ($P_{BoP,fc}$) and the battery BoP ($P_{BoP,bat}$). P_{aux} (kW) is the same for every propulsion system analyzed. They include heating, ventilation, and air conditioning of the indoor environment, sockets, and lighting. The outdoor temperature heavily influences the heating/cooling power demand of the wagons. For this case study, an outdoor temperature equal to 15 °C is set for the case study, with an average auxiliary requested power of around 90 kW. Equation (10) shows how the dynamic behavior of the FC is controlled, imposing maximum ramp-rates to the current to slow the aging of the component.

$$\left(\frac{dI}{dt}\right)_{min} \le \frac{dI_{fc}(t)}{dt} \le \left(\frac{dI}{dt}\right)_{max} \tag{10}$$

The set of Equation (11) explains how the battery system is modeled:

$$\begin{cases} P_{bat}(t) = \left(P_{load}(t) + P_{aux}(t) + P_{BoP}(t) - P_{fc}(t) \cdot \eta_{conv}\right) \cdot \varphi \\ -C_{charge} \cdot BAT_{cap} \le P_{bat}(t) \le C_{discharge} \cdot BAT_{cap} \end{cases} \tag{11}$$

P_{bat} (kW) is the power that the battery exchanges with the traction system. It can be calculated as the difference between the power demand of the system and the power supplied by the FC. A positive value means that the power is withdrawn from the battery, while a negative value means that the battery is being charged. Additionally, the battery power is limited by maximum and minimum values related to the charging and discharging rates (C_{charge}, $C_{discharge}$). η_{bat} is the battery efficiency, and φ is a variable that can assume two values, depending on battery operating state (charging or discharging), as shown in Equation (12).

$$\varphi = \begin{cases} \dfrac{1}{\eta_{bat}}, if\ P_{bat} > 0 \\ \eta_{bat}, if\ P_{bat} \le 0 \end{cases} \tag{12}$$

The state of charge is calculated every instant of time, as shown in Equation (13): SoC_o is the initial state of charge of the battery, which must be equal to the state at the end of the route due to the energy system's control strategy.

$$SoC(t) = SoC_o - \frac{\int_0^t P_{bat}(t) \cdot dt}{BAT_{cap}} \tag{13}$$

2.2.3. Fuel consumption

For all the propulsion systems, the fuel consumption of the route, q_{fuel} (kg or l), can be calculated by dividing the total chemical energy spent (E_d) by the lower heating value (LHV) of the fuel used (LHV, 33.3 kWh/kg for hydrogen and 10.7 kWh/l for diesel).

$$q_{fuel} = \frac{E_d}{LHV} \tag{14}$$

Finally, by dividing the total fuel consumption by the route length l (km), the specific fuel consumption $\dot{q}_{fuel}$ (kg/km or l/km) can be evaluated:

$$\dot{q}_{fuel} = \frac{q_{fuel}}{l} \tag{15}$$

This last parameter is very important to compare propulsion systems that use different fuels since it gives immediate feedback of which is the

Table 2
Specific costs of electrification infrastructure [25,26].

Electrification difficulty	Cost [M€/km]	Lengths on the Brescia-Iseo-Edolo [km]
Easy	2	91.4
Difficult	10	11.6

Table 3
Access fee costs of a regional railway [27].

Parameter	Value [€/km]
A_1	0.136
A_2	0.125
A_3	0.0 no pantograph (HMU, DMU) 0.024 with one pantograph (EMU)
B	3.091

most energy saving alternative.

The chemical energy given by the main energy source (E_d) is evaluated as detailed in the following section.

2.2.3.1. Hydrogen Multiple Unit (HMU). Concerning the HMU, once the power contributions from the fuel cell and the battery are defined, the overall energy demand of the route can be evaluated and coincides with the energy exiting the fuel cell. This energy (E_{d-HMU}, in kWh) can be calculated as in Equation (16).

$$\begin{cases} P_{H_2}(t) = \dfrac{P_{fc}(t) - P_{BoP,fc}(t)}{\eta_{syst}(t)} = \dot{m}_{H_2}(t) \cdot LHV \\ E_{d-HMU} = \displaystyle\int_0^{t_{end}} P_{H_2}(t) \cdot dt \end{cases} \tag{16}$$

P_{H_2} (kW) is the power of the hydrogen stream and it is calculated as the total instantaneous electrical power generated by the FC, divided by the FC system efficiency η_{syst}, that already considers the balance of plant of the FC ($P_{BoP,fc}$) and for this reason must be subtracted from the total. It can be expressed as the mass flow rate of hydrogen $\dot{m}_{H_2}$ (kg/s) times the LHV. Then the P_{H_2} can be integrated to find the total energy (q_{fuel} and E_{d-HMU}) consumed along the route.

2.2.3.2. Diesel multiple unit (DMU). To build a model that estimates the overall energy demand of the DMU starting from the evolution of traction force over time, the train currently in use on the Brescia-Iseo-Edolo route, the ATR 125, has been chosen. This train does not include a battery system. While the main train's specifications are well-known and shown in Table 8, since it is a commercial passenger train, operational parameters (e.g., efficiency curves, fuel consumption, and traction parameters) are not publicly available. For this reason, a practical method to calculate DMU's efficiency has been adopted from literature [22]. Equation (16) can be simplified and the energy consumption of the DMU (E_{d-DMU}, in kWh) can be calculated as in Equation (17). Here η_{W-DC} stands for the wheel-to-DC-bus efficiency, accounting for losses associated with the transmission of mechanical and electrical power. η_{DC-T} is the DC-bus-to-tank efficiency and considers the losses related to mechanical power generation and its conversion into electricity.

$$E_{d-DMU} = \int_0^{t_{end}} \frac{P_t(t) + P_{aux}(t)}{\eta_{W-DC}(t) \cdot \eta_{DC-T}(t)} \cdot dt \tag{17}$$

2.2.3.3. Electric Multiple Unit (EMU). Regarding the EMU, the decision was made to rely on energy consumption data from existing literature. This approach was chosen because – for the selected case study – EMUs incur minimal costs for the electricity they consume [23], making a detailed energy consumption model unnecessary since – in this context – building an accurate model would have little impact on the overall economic analysis.

Table 4
PEMFC operative specifics.

Characteristics	Symbol	Value	Ref.
Maximum current ramp-up [A/s]	$\left(\frac{dI}{dt}\right)_{max}$	15	Assumed
Maximum current ramp-down [A/s]	$\left(\frac{dI}{dt}\right)_{min}$	−60	[28]
FC BoP contribution [%kW]	–	CONFIDENTIAL	

Table 5
NMC-G battery parameters.

Characteristics	Value	Ref.
SoC range [%]	80–20	Assumed
Max C rate discharge [−]	3.0	[32]
Max C rate charge [−]	1.8	[32]
Battery BoP [kW]	CONFIDENTIAL	

2.3. Techno-economic analysis

In order to compare the different propulsion system technologies, a techno-economic analysis is essential, as it considers the costs over the entire lifetime of the train. To evaluate the economic viability of the different propulsion methods, the TCO parameter has been calculated, incorporating capital costs (CAPEX, in €) and operational costs (OPEX, in €/year). The TCO allows for easy comparison of different train propulsion systems and configurations by providing a cost-per-kilometer output (€/km). The analytical formula is provided in Equation (18).

$$TCO = \frac{CAPEX + \sum_{t=1}^{N} \frac{OPEX}{(1+r)^t}}{\sum_{t=1}^{N} \frac{ADT}{(1+r)^t}} \tag{18}$$

r is the discount rate, chosen equal to 5 % and N is the number of years of the analysis (25 for the trains [24] and 30 for the catenary) and t ranges from 1 to N. ADT is the annual traveled distance (km/year).

2.3.1. CAPEX

The CAPEX is found as the sum of all the capital costs involved, seen as the product of the specific costs and the sizes of the components, as described in Equation (19).

$$CAPEX = \sum_{i=1}^{B} (n_i \cdot c_i \cdot S_i + C_i) \tag{19}$$

where c_i is the specific cost of the i-th component (€/kW, €/kWh, €/kg, etc.), S_i is its size (kW, kWh, kg, etc.) and n_i is the number of elements of the component. C_i are the absolute costs that do not scale with the size (€) and B is the number of purchased components.

$$OPEX = \sum_{y=1}^{B} (c_y \cdot ADT + C_y + C_{rep,y}) \tag{20}$$

The OPEX costs are divided into.

Table 6
Transmission system parameters of the trains.

Parameter	Symbol	Value	Ref.
Gear efficiency [%]	η_{gear}	97.5	Assumed[a]
DC-DC converter efficiency [%]	η_{conv}	98.0	Assumed[a]
Electric motor efficiency [%]	η_{motor}	94.0	Assumed[a]
Regenerative braking velocity threshold [km/h]	–	8.0	[21]

[a] Product of η_{gear}, η_{conv} and η_{motor} similar to other works in literature [21,33].

Table 7
CAPEX and OPEX calculation input data of the HMU.

CAPEX parameters	Value	Ref.
Specific costs		
c_{pm} [€/kW]	1200	[35,36]
c_{BAT} [€/kWh]	350	[36,37]
c_{tank} [€/kgH_2]	600	[38]
Absolute parameters [a]		
Range [km]	>600	[39]
n_{pm} [−]	2	[17]
PM_{size} [kW]	200	From Section 5.1
BAT_{cap} [kWh]	425	From Section 5.1
n_{BAT} [−]	2	[17]
C_{et} [€]	7e6	Assumed
OPEX parameters	**Value**	**Ref.**
Specific costs		
$c_{m\&r}$ [€/km]	0.85	[40]
c_{PMdA} [€/km]	3.353	[27]
c_{fuel} [€/kg]	8.00	[34]
Absolute parameters		
C_{salary} [€/year]	128,000.00	[41]

[a] FC replacement: full every 10 years (100 % CAPEX), mild every 5 years (33 % CAPEX [42]), resulting in a substitution every 5 years [40]; Battery replacement: Full every 8 years (100 % Capex) [40]. These costs will be considered in the CAPEX.

Table 8
ATR 125 specifics.

Characteristics	Value	Ref.
Weight [ton]	134	[43]
Max speed [km/h]	140	[43]
Power [kW]	1528	[43]

- Variable operating costs, expressed as a function of the traveled distance. The term c_y is the specific expenditure (€/km).
- Fixed operating costs, which do not depend on the traveled distance. The term C_y expresses the annual operative costs, directly expressed as €/y.
- $C_{rep,y}$ (€) is the replacement cost of the component *i* that occurs in the year in which it is substituted.

The CAPEX can be calculated as shown in Equation (21).

$$CAPEX = n_{pm} \cdot c_{pm} \cdot PM_{size} + n_{bat} \cdot c_{bat} \cdot BAT_{cap} + c_{tank} \cdot m_{fuel} + C_{et} + C_{OH} \quad (21)$$

c_{pm} (in €/kW) and c_{BAT} (in €/kWh) are the specific costs respectively of the main energy source (i.e., prime mover) and the battery (if present), while – since the train under study is a multiple unit – n_{pm} is the number prime movers and n_{BAT} is the amount of battery packs. PM_{size} is the size of the single module of the prime mover (in kW) and BAT_{cap} is the capacity of the battery pack (in kWh). The c_{tank} (in €/kg or €/l) is the specific cost of the storage per unit of fuel (only for HMU and DMU) that needs to be multiplied by m_{fuel}, which is the quantity of fuel able to reach the expected daily range (kg or l). The C_{et} (in €) is the cost of the empty train, so the train without the energy storage and propulsion system. C_{OH} (€) is the cost to electrify the line and is considered just for the EMU case. It can be calculated as:

$$C_{OH} = \sum_{x=1}^{2} c_x \cdot L_x \quad (22)$$

Equation (22) states that c_x is the specific cost of electrification and can have two different values depending on the difficulty to electrify the line, as Table 2 shows. L_x is the length of the segments for each difficulty.

2.3.2. OPEX

According to Equation (20), the OPEX is evaluated as the annual expenditure that the train requires. Starting from Equation (20), the OPEX can be detailed as:

$$OPEX = \left(c_{m\&r} + c_{fee} + c_{fuel} \cdot \dot{q}_{fuel}\right) \cdot ADT + C_{salary} \quad (23)$$

where the $c_{m\&r}$ is the maintenance and reparation cost of the powertrain (in €/km) which includes the maintenance and the eventual substitution of the powertrain's components, c_{fuel} is the cost of fuel (€/kgH_2, €/l or €/kWh) and c_{fee} is the access fee that the company must pay to use the infrastructures as the railway (in €/km). It is defined in accordance with the provisions of art. 13 of Legislative Decree no. 112/15 and, precisely, in par. 5.1, as:

$$c_{fee} = A_1 + A_2 + A_3 + B \quad (24)$$

A_1 regards the unit prices by weight class of the train, A_2 is unit price by operating speed. For the A_3 fee section – since there is not a specific class for hydrogen trains – the diesel fee is considered since the HMU does not use the pantograph line. The coefficient B of the access charge is related to the market segments' ability to pay. The values of these parameters can be found in Table 3.

The specific costs are then multiplied by ADT in order to find the annual expenses. C_{salary} is the gross salary of the on-board staff of the train (in €/year). All the input parameters of the propulsion systems used to calculate the TCO are grouped in Section 3.

3. Propulsion systems breakdown

A detailed breakdown of the propulsion systems analyzed in the present study is shown in the following sections. Each layout is explained in terms of its components and energy requirements.

3.1. Hydrogen Multiple Unit

The main components of an HMU include a fuel cell as the prime mover, a battery energy storage to increase the system responsiveness, a DC-DC converter, the Balance of Plant (BoP) for both the fuel cell and the battery, and the fuel tank. The interaction between the components can be found in Fig. 3.

3.1.1. Fuel cell system

The HMU uses hydrogen-powered PEMFC as the prime mover to harvest the high fuel-to-electricity conversion and to reduce the local emissions of the train. Its characteristics are shown in Table 4.

The fuel cell system requires various BoP components for proper operation. These primarily include systems for hydrogen supply, air supply, temperature regulation, water management, and power electronics for control. The state of health of the fuel cell is evaluated under Medium of Life (MoL) conditions to improve the accuracy of fuel consumption estimation for the HMU. According to Ref. [29], for PEMFCs, the average degradation rate of energy efficiency is 0.88 % per 1000 h of operation under dynamic conditions. Moreover, maximum ramp-down and ramp-up values for the current are considered to preserve the FC life, and can be seen in Table 4. The ramp-up value has been assumed starting from internal know-how and other literature works [28]) Regarding the TCO analysis, assuming a substitution of the fuel cells every five years, the total degradation at End of Life (EoL) would be 23.12 %, with an average efficiency degradation of 11.56 %. This value is considered as hydrogen consumption increase compared to the Beginning of Life (BoL) case, and so resulting in a decrease of the efficiency of the cell, as shown in Fig. 4c. The efficiency of the FC system at MoL reaches a maximum of about 47 % close to 25 % of the rated power, with an efficiency of approximately 35 % at rated conditions. This efficiency curve is based on the lower heating value (LHV).

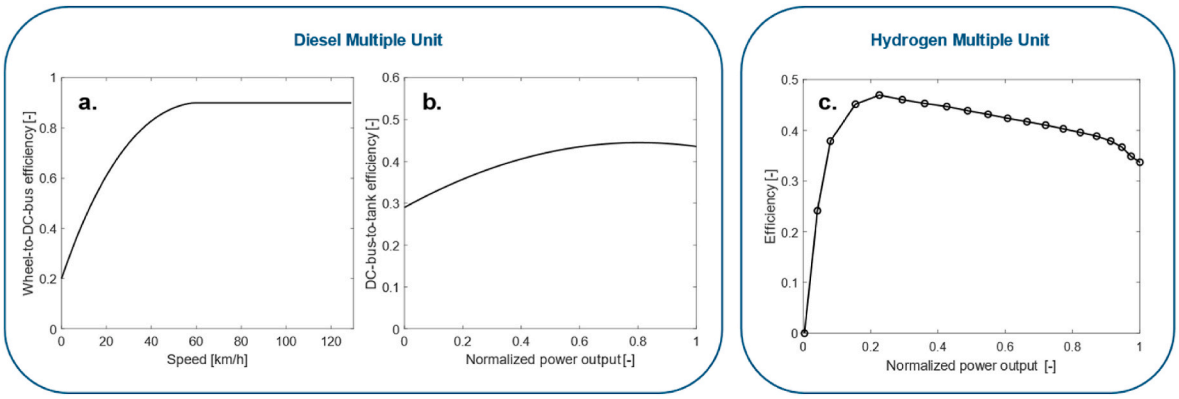

Fig. 4. a) Wheel-to-DC-bus efficiency as a function of the train's speed; b) Estimated DC-bus-to-tank efficiency as a function of the normalized power output [22]; c) System fuel cell efficiency η_{syst} at Medium of Life (MoL) based on LHV. Normalized power output corresponds to the ratio between the fuel cell's actual power and the rated power, and it ranges from 0 to 1.

3.1.2. Battery energy storage system

To cover the high-power demand phases, a traction energy battery for heavy-duty vehicles is considered. The battery is an NMC-Graphite and has maximum charge-discharge rates (C-rates) that are shown in Table 5 together with other technical parameters. This battery has been evaluated based on the existing commercial relationship between Alstom and Leclanché, as well as Leclanché's collaboration with Cummins. This partnership demonstrates their commitment to integrating their battery cells with hydrogen fuel cells for trains ([30,31]).

Regarding the battery's BoP, a cooling circuit is needed to keep the right operational temperature. It consists of a pump for water circulation and a heat pump to control the primary fluid temperature.

3.1.3. Transmission system parameters

The parameters of the power transmission system of the HMU are shown in Table 6. They are fundamental for both the traction and the regenerative braking phases.

3.1.4. HMU economic parameters

Regarding the TCO calculation – explained in Section 2.3 – the CAPEX and OPEX parameters can be found in Table 7. The fuel consumption ($\dot{q}_{fuel}$) is an output of the model and is detailed in Section 5.2. The hydrogen price (c_{fuel}) is assumed to be the base case price and equal to €8/kg, which is close to the suggested production costs of hydrogen in Europe for 2023 by water electrolysis utilizing grid electricity (€7.94/kg [34]).

Table 9
CAPEX and OPEX calculation input data of the DMU.

CAPEX parameters	Value	Ref.
Specific costs		
c_{pm} [€/kW]	670	Includes: Engine and generator [45]; Inverter [46]
c_{tank} [€/l]	negligible	–
Absolute parameters		
n_{pm} [−]	4	Assumed
PM_{size} [kW]	382	[43]
C_{et} [M€]	7.00	Assumed
OPEX parameters	**Value**	**Ref.**
Specific costs		
$c_{m\&r}$ [€/km]	1.05	[40]
c_{PMdA} [€/km]	3.353	[27]
c_{fuel} [€/kg]	1.234	[44]
Absolute parameters		
C_{salary} [€/year]	128,000.00	[41]

3.2. Diesel multiple unit

The chosen DMU train is the ATR 125, since it the train actually used on the case study's line. In Table 8 its specifics are shown.

Regarding the DMU's methodology to calculate the traction profile, it is the same as the one explained in Section 2.2.1, but the chemical energy is found by passing through a Wheel-to-DC-bus efficiency (η_{W-DC}) and then going backward through a DC-bus-to-tank efficiency (η_{DC-T}) as Equation (17) explains, according to Ref. [22]. In Fig. 4 the evolution of the efficiencies used in Equation (17) are shown.

3.2.1. DMU economic parameters

Regarding the DMU economic parameters, Table 9 provides a complete breakdown of the costs. It is important to note that the fuel cost c_{fuel} is the average price of diesel, subtracted by the taxes [44].

3.3. Electric Multiple Unit

When the EMU is analyzed – as previously anticipated – it was decided to use specific energy consumption data from existing literature. This approach was chosen because the low electricity costs of EMUs make developing a detailed energy consumption model unnecessary. The EMU consumes 8.5 kWh of electricity for each km [40].

Table 10
CAPEX calculation input data of the EMU.

CAPEX parameters	Value	Ref.
Specific costs		
c_{pm} [€]	100,000.00	Assumed
c_{tank} [€/l]	n/a	–
Absolute parameters		
n_{pm} [−]	1	Assumed
PM_{size} [kW]	n/a	–
C_{et} [M€]	7.00	Assumed
OPEX parameters	**Value**	**Ref.**
Specific costs		
$c_{m\&r}$ [€/km]	CONFIDENTIAL (line) + 0.725 (train)	[40]
c_{PMdA} [€/km]	3.377	[27]
c_{fuel} [€/kWh]	0.003	[23]
Absolute parameters		
C_{salary} [€/year]	128,000.00	[41]

3.3.1. EMU economic parameters

The EMU economic parameters are provided in Table 10. In this case, the propulsion system CAPEX is less onerous than the other propulsion systems. It has to be highlighted that the cost of electricity c_{fuel} is much cheaper than the other cases, suggesting that this cost will have not much impact on the final TCO.

4. Case study: Brescia-Iseo-Edolo

To enable the tool to provide some comparative results, the Brescia-Iseo-Edolo railway line is selected for the analysis as a case study. Its characteristics are shown in Table 11. This non-electrified, single-track line is located in Valcamonica, Northern Italy. Currently, electric DMUs (ATR 125) are being used, which Trenord – in collaboration with Alstom – plans to replace with 14 high-efficiency HMUs [47].

The line altitudes and the simulation results are shown in Fig. 5. The latter indicate significant power variations throughout the mission, highlighting the necessity of integrating batteries to support fuel cell use on trains. The battery system enhances the powertrain's dynamic behavior, enabling it to meet the steepest load changes along the route. During the braking phase, the power experienced by the wheel is predominantly negative. This characteristic allows the energy system to efficiently recover energy in the battery through regenerative braking, significantly reducing the train's fuel consumption, as demonstrated in Section 5.2.

5. Results and discussion

In Section 5.1, the optimal sizing of the powertrain is presented through a minimization of the TCO. Section 5.2 shows the results of the simulation by comparing the energy consumption performances of the three propulsion systems (HMU, DMU, EMU). Section 5.3 examines the economic outcomes of the analysis, while Section 5.4 analyzes how fuel prices influence the cost-effectiveness of the different propulsion systems.

5.1. Optimization of the HMU size

A sensitivity analysis on the hybridization ratio of the HMU's powertrain (i.e. the ratio between the rated power of fuel cell and battery) was conducted to fix the optimal sizes of FC and batteries for the selected case study. The analysis examined the full range from a battery-only propulsion system (0 % hybridization ratio) to a FC-only propulsion system (100 % hybridization ratio). Fig. 6 presents the optimization analysis map, showing the TCO as a function of the hybridization ratio.

The simulation considers several constraints to delineate non-feasible regions in the optimization map. The feasibility region (highlighted in green in Fig. 6) is defined by the following constraints.

1. The powertrain must complete the route satisfying the energy and power needs of the mission.
2. The train must be capable of accessing the refueling station/charging station only once per day.
3. The powertrain's maximum weight-per-axle must not exceed 18 t/axle.
4. The powertrain must satisfy the *SoC* constraint (charge-sustaining mode, i.e. the state of charge at the end of the route should be the same as at the beginning of the route).

Table 11
Brescia-Iseo-Edolo input data.

Parameters	Value
Maximum height difference [m]	527.6
Maximum slope [‰]	26.0
Mean slope [‰]	3.44
Track length [km]	102.7
Number of stations	24
Max speed [km/h]	$\leq$ 90 (variable)

Design conditions that fail to meet major constraints (1-3) are marked in red, while configurations that violate minor constraint (4) are shown in yellow. In Fig. 6, the global optimal hybridization ratio (marked by a light-blue diamond, TCO €10.45/km) lies within the yellow region, indicating that it would not operate in self-sustaining mode. As a result, this global optimum is considered not acceptable. Instead, a local minimum located within the feasibility region is identified (marked by a light-blue circle, TCO €10.80/km). Table 12 presents the optimal sizes of the HMU components, which will serve as the basis for subsequent analysis.

It is also worth highlighting the behavior of the TCO in the first half of the feasibility region (between about 25 % and 45 %), since the TCO curve appears to be flat. This plateau permits a small range of hybridization in a region of quite constant TCO in order to meet the requests of the route: flatter routes may require less batteries on board, while a more energy-intensive one may require more. Following the behavior of the curve on the right side of the graph, the TCO rapidly increases due to a higher hydrogen consumption – given by the oversizing of the FC that affects the operating point and increases the mass – and by the powertrain's cost. The feasibility here is not matched since the rapid power changes may not be satisfied by the hybrid system due to the small battery's dimensions and the FC's constraint on the maximum ramp-up rate. The results also show that the sizes of the powertrain are very similar to the one of the real case study, demonstrating that the train has been well designed for the route.

5.2. Fuel consumption comparison

Once the optimal sizes of the HMU have been found, a comparison of the HMU solution with alternative propulsion systems (DMU and EMU) can be made. The results show how high-efficiency conversion systems such as fuel cells and batteries can successfully complete an energy-consuming route like the one under study.

The main outcomes from the energy analysis of the different propulsion options are provided in Table 13. These results are essential in order to estimate the operational costs of the train in the TCO analysis that is carried out in Section 5.3. Table 13 shows that the DMU – for this specific case study and based on the assumptions previously discussed – is the option with the lower average propulsion system efficiency, with a chemical energy consumption that is 1.9–2.8 times higher than the other two cases.

Fig. 7 illustrates the evolution of some of the most important parameters of the HMU over the course of the trip (with fuel cell data shown in red and battery data in black). As shown in Fig. 7a, the hydrogen consumption is higher on the outward journey and lower on the return due to the slope of the line. Fig. 7b displays the SoC of the battery, confirming the effectiveness of the charge-sustaining operating mode. Fig. 7c shows the power contributions from both the battery and the fuel cell during the trip. These results highlight the importance of an effective energy management strategy for the propulsion system: the battery satisfies all the steepest power variations of the train linked to the departures from the stations (positive peaks) and the braking phases (negative peaks), making it the major power source and permitting energy recovery through regenerative braking. Contrarywise, the FC acts as range extender, enabling the use of a smaller battery and thereby reducing both capital and operational costs.

5.3. Total cost of ownership outcomes

The TCO for the three propulsion systems – HMU, DMU, EMU – operating in the Brescia-Iseo-Edolo route is illustrated in Fig. 8a, revealing key cost distribution insights for each system. The TCO

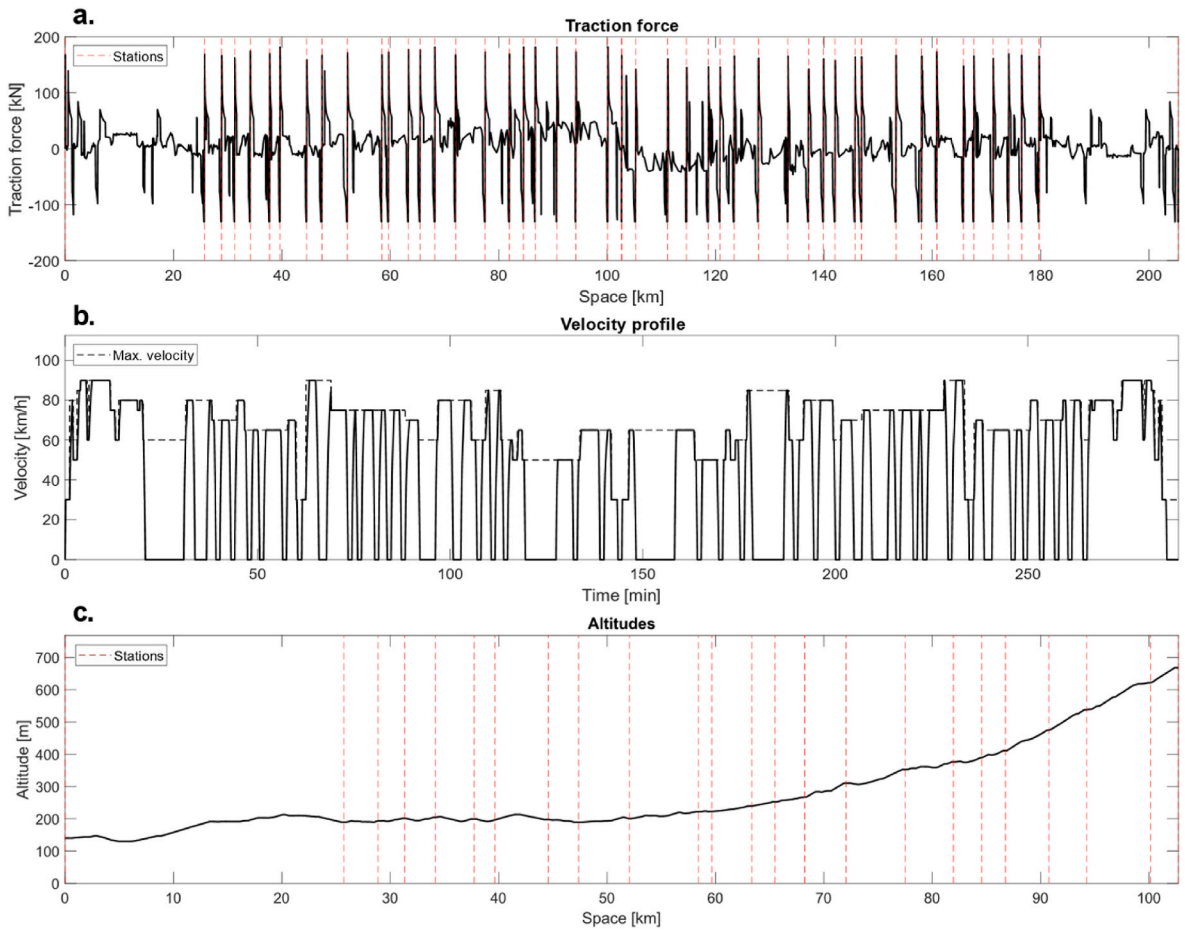

Fig. 5. a) Traction force of the HMU along the Brescia-Iseo-Edolo route; b) Velocity profile along the route; c) Experienced altitude variation.

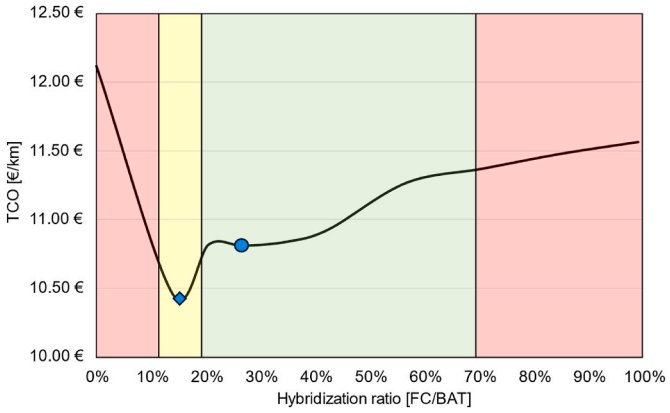

Fig. 6. Size optimization results of the powertrain. Red regions indicate that one of the major requirements is not satisfied (constraints 1-2-3); the yellow region indicates that a minor constraint is not satisfied (constraint 4), green region represents the feasibility region where all constraints are met. The light-blue dot indicates the local optimal hybridization ratio, while the light-blue diamond is global optimal hybridization ratio. (For interpretation of the references to colour in this figure legend, the reader is referred to the Web version of this article.)

Table 12
Results of the optimization analysis of the HMU size.

Characteristics	Value
FC size [kW]	400
Battery size [kWh]	850
Local optimal TCO [€/km]	10.80

Table 13
Energy-related outcomes and assumptions of the Brescia-Iseo-Edolo route (back-and-forth).

Parameters	HMU	DMU	EMU
Energy consumption [kWh]	2591	4827	1746
Fuel consumption [kgH_2; l; kWh]	77.8	451.1	1746
Specific fuel consumption [kgH_2/km; l/km; kWh/km]	0.38	2.20	8.0 [40]
Average ageing contribution [kgH_2/km]	0.04 [29]	0	0
SoC roundtrip variation [%]	0.0	n/a	n/a[a]
Average propulsion system efficiency [%]	41.4	26.4	72.9

[a] n/a: not applicable.

breakdown shows substantial variation across the three systems, with each being influenced by different cost components.

- **HMU**: For hydrogen-powered trains, fuel costs are the second largest contributor at €3.36/km (31 % of TCO), reflecting the current economic impact of hydrogen as an energy vector. Salary and access fees combine for €3.92/km, accounting for 36 % of the total. Maintenance and repair costs, though relatively minor at €0.85/km, are still crucial for vehicle reliability. The propulsion system cost (€0.47/km) is the highest among all the solutions since a periodic replacement of the components is considered (fuel cells and batteries). Together with the propulsion system cost, the CAPEX associated with

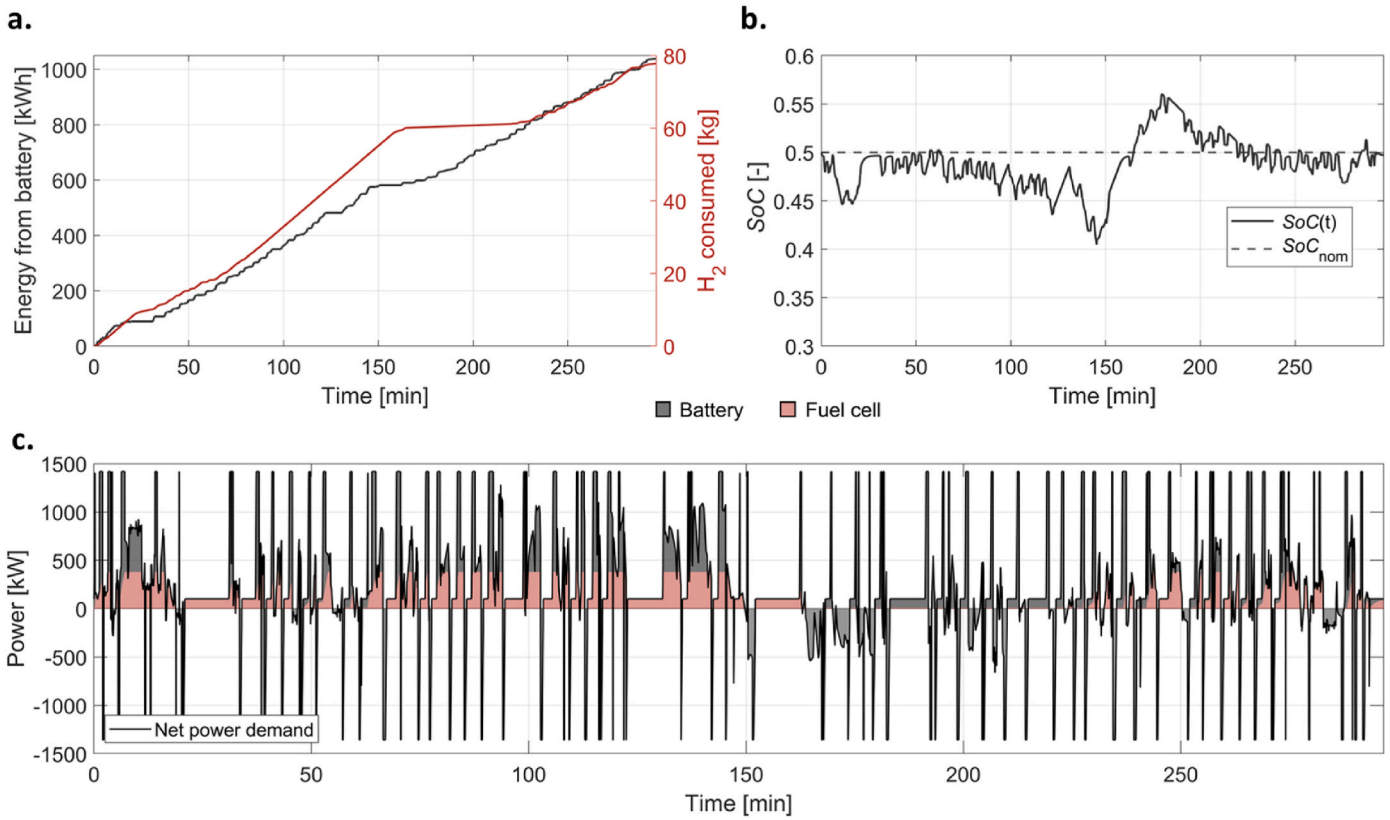

Fig. 7. Simulation results of the HMU. a) Monitoring of the energy consumption of the propulsion system; b) State of Charge of the battery over time; c) Net power contribution breakdown from different sources. Tuning ECMS parameters for the current case study are: $k_p = -12$, $k_a = 300$, $n = 3$. In red the behavior of the fuel cell, in black the battery. (For interpretation of the references to colour in this figure legend, the reader is referred to the Web version of this article.)

the purchase of the trains represents only the 25 % of the TCO, demonstrating the importance of a life cycle cost approach. These elements bring the total TCO for hydrogen trains to €10.80/km.

- **DMU**: Diesel propulsion, on the other hand, presents a slightly lower total TCO of €10.21/km. This reduction is largely due to lower fuel costs at €2.71/km, compared to hydrogen, despite the lower efficiency of the technology. However, as for HMU, salary and access fees remain a significant factor at €3.92/km. Maintenance and repair expenses stand at €1.05/km, higher than the HMU case due to the presence of moving parts in the power generation path. The lower fuel cost – thanks to the big cut of taxes on the fuel – help position diesel propulsion as a more cost-effective option than hydrogen, in the current scenario and for the specific case study under evaluation.
- **EMU**: Electrification overhead, representing the cost structure for fully electrified rail, shows the highest TCO close to €14/km, driven mainly by the high costs associated with infrastructure construction (particularly high for the selected case study). Indeed, the electricity costs are very low for regional trains (i.e. the one investigated in this work) and so are negligible and have minimal impact on total expenses, while electrification infrastructure contributes €6.16/km, making it the most substantial cost contribution across all three options. This is mainly given by the high cost to electrify the line, mainly driven by the presence of many hindrances such as tunnels and bridges. A higher volume of traffic on the line would reduce this cost. Even the maintenance cost are high, since they include both the train's and the line's costs. Salary and access fees remain similar at €3.95/km, slightly higher due to the presence of the line contact, while maintenance and repair costs are in line with the HMU.

5.4. Sensitivity analysis on fuel prices

The sensitivity analysis shown in Fig. 8b explores the impact of variable fuel prices (hydrogen price for HMU, and diesel price for DMU) on the TCO of different propulsion systems. For each combination of hydrogen and diesel prices, the figure highlights the optimal powertrain solution in terms of TCO (according to the assumptions discussed above) and highlights the weight of fuel prices on the total cost.

These results indicate that for scenarios where hydrogen prices are below €5–6/kg and the mean diesel prices are above €1.2–1.3/l, the HMU is likely to emerge as the most competitive solution to decarbonize non-electrified railways lines, such as the one investigated in this work. The most probable scenario of prices is represented with a zoom on the left side of Fig. 8b. Additionally, for this specific train route, the EMU is found to be a viable alternative only under very high fuel price conditions that appear to be unrealistic (top-right side of the complete matrix, in grey). This consideration applies to routes characterized by low traffic volumes and numerous bridges and tunnels, which make the investment cost for electrification extremely high.

6. Conclusions

This study introduces a comprehensive modeling framework designed to simulate the train and route dynamic, integrated with the model of novel hydrogen-powered trains (HMU). The framework allows energy and economic comparisons with conventional propulsion systems, such as diesel (DMU) and electric (EMU) trains. A key advantage of this modeling tool lies in its applicability to any railway line, achieved through a flexible structure that accounts for specific route characteristics, such as slopes and maximum speed limits. Additionally, the tool allows for the optimization of HMU's system components (fuel cells and batteries, in this case 400 kW total fuel cell size and 850 kWh battery capacity), enabling tailored analysis for different operational conditions. This capability makes the developed framework an effective solution for guiding decarbonization strategies and decisions in the rail transport

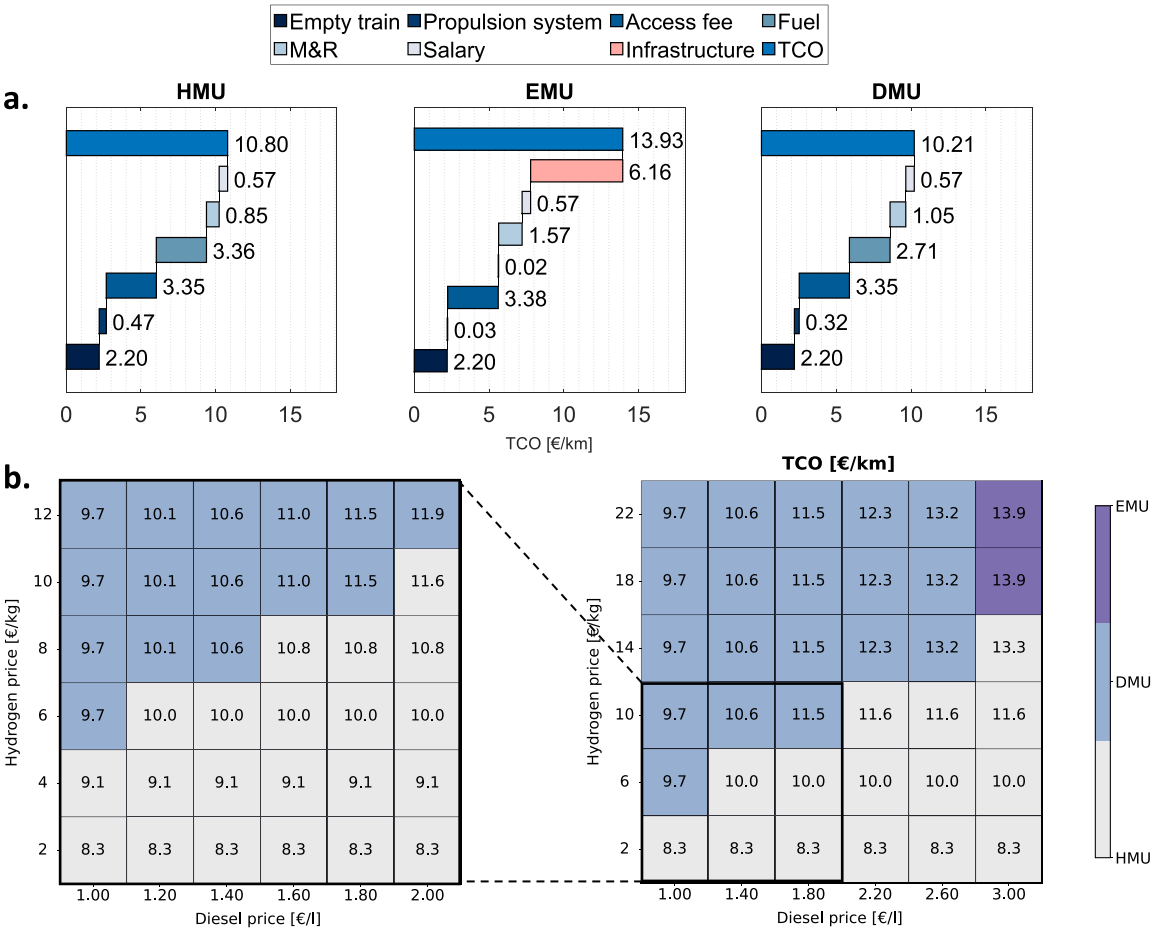

Fig. 8. a) TCO results for HMU, EMU and DMU trains for the Brescia-Iseo-Edolo line; b) Sensitivity analysis on fuel prices (the EMU benefits from a low fixed electricity price equal to 0.3 c€/kWh): the x-axis represents the diesel price, while the y-axis represents the hydrogen price. The left image provides a zoomed-in view of typical fuel prices, highlighting the most likely scenarios.

sector.

The in depth-study conducted on the Brescia-Iseo-Edolo line demonstrates that HMUs present a future promising and sustainable alternative to conventional DMUs and EMUs when long and non-electrified lines with many difficulties in electrification are present. By integrating hydrogen fuel cells and batteries, HMUs not only avoids direct greenhouse gas emissions but also enhance energy efficiency and operational flexibility, making them suitable for non-electrified rail routes with challenging terrains. The TCO analysis revealed that, for the chosen case study, diesel propulsion remains slightly more cost-effective due to lower fuel prices and mature infrastructure (€10.21/km) with the HMU close behind (€10.80/km), with a gap of 6 % which is in line with the Roland Berger's study [12]. However, the situation is likely to change with rising diesel costs and the expected reduction in hydrogen prices, which will make HMUs increasingly competitive for the selected train route. The sensitivity analysis supports this conclusion, indicating that hydrogen-powered trains' TCO is highly affected by the cost of hydrogen and a breakeven price of €5/kg can be found for the selected case study. This means that below this price, HMU is the best option on the presented line, according to actual prices of diesel.

The EMU presents the highest TCO (€13.93/km) due to the high infrastructure's cost. Future work will build upon the model developed in this study to investigate the optimal trade-off between hydrogen price trajectories and fuel cell replacement strategies, with the goal of minimizing overall lifecycle costs. Additionally, the same route will be used to explore alternative energy management strategies, in order to assess their impact on system performance and cost. The framework will also be applied to other railway lines to identify the most suitable propulsion configurations for different operational contexts.

CRediT authorship contribution statement

Gabriele Peyrani: Writing – original draft, Visualization, Software, Methodology, Investigation, Formal analysis, Data curation, Conceptualization. **Paolo Marocco:** Writing – review & editing, Supervision, Project administration, Investigation, Formal analysis, Conceptualization. **Marta Gandiglio:** Writing – review & editing, Visualization, Supervision, Project administration, Investigation, Conceptualization. **Pierpaolo Cherchi:** Writing – review & editing, Validation, Supervision, Resources, Project administration, Methodology, Data curation, Conceptualization. **Massimo Santarelli:** Writing – review & editing, Supervision, Project administration, Funding acquisition, Conceptualization.

Declaration of competing interest

The authors declare that they have no known competing financial interests or personal relationships that could have appeared to influence the work reported in this paper.

7. Acknowledgements

This paper and the results presented are based exclusively on estimates deduced by the authors, based on the documents indicated in the

bibliography. The analysis was conducted independently, without the involvement of FNM or companies related to it, which is therefore external to the discussion itself. This research was funded by the European Union - Next Generation EU – Project ID: IPCEI-I1_0000003 CUP: B19J23000490004 coordinated by Alstom Ferroviaria S.p.A.

Acronyms

Acronym	Meaning
ADT	Annual Traveled Distance
BoL	Beginning of Life
BoP	Balance of Plant
CAPEX	Capital Costs
DMU	Diesel Multiple Unit
ECMS	Equivalent Consumption Minimization Strategy
EMS	Energy Management Stategy
EMU	Electric Multiple Unit
EoL	End of Life
FC	Fuel Cell
HMU	Hydrogen Multiple Unit
LHV	Lower Heating Value
MoL	Medium of Life
NSGA	Non-Dominated Sorting Genetic Algorithm
OPEX	Operational Costs
PEMFC	Proton Exchange Membrane Fuel Cell
RB	Rule Based
SoC	State of Charge
TCO	Total Cost of Ownership

Symbols

Symbol	Meaning	Units
$A-B$	Unit prices of the access fee	€/km
a	Acceleration	m/s^2
BAT_{cap}	Battery capacity	kWh
b	Rolling resistance	N/(km/h)
C	C-rate	1/h
C_i	Absolute costs	€
c	Aerodynamic resistance	N/(km/h)^2
c_i	Specific costs	€/kW-€/kWh-€/kg-€/l
E_d	Energy consumption	kWh
e	Static resistance	N
F	Force	N
FC_{size}	Fuel cell size	kW
g	Gravitational acceleration	m/s^2
I	Current	A
k_p, k_a, n	Tuning parameters	–
L_x	Line length	km
M	Mass	t
$\dot{m}_{H_2}$	Specific hydrogen consumption	kg/s
n_i	Number of components	–
N	Number of years	–
P	Power	kW
PM_{size}	Prime mover's size	kW
q_{fuel}	Amount of fuel consumed	kg-l-kWh
$\dot{q}_{fuel}$	Specific fuel consumption	kg/km-l/km-kWh/km
R	Resistive force	N
r	Discount rate	%
s	Space	m
S	Sizes	kW-kg-kWh
t	Time	s
v	Velocity	m/s
α	Slope	–
η	Efficiency	–
λ	Rotary allowance	–
φ	Charging - Discharging efficiency	–

Data availability

Data will be made available on request.

References

[1] Eurostat, Length of railway lines by number of tracks and electrification of lines [Online]. Available: https://ec.europa.eu/eurostat/databrowser/view/rail_if_line_tr_custom_10150374/bookmark/table?lang=en&bookmarkId=6376f091-4a12-4608-a089-4f698c265c1a. (Accessed 3 October 2024).

[2] Joint Research Center, Batteries for Energy Storage in the European Union, 2022, https://doi.org/10.2760/808352.

[3] D. Gattuso, A. Restuccia, A tool for railway transport cost evaluation, Proced. Soc. Behav. Sci. 111 (Feb. 2014) 549–558, https://doi.org/10.1016/j.sbspro.2014.01.088.

[4] P. Fragiacomo, F. Piraino, Numerical modelling of a PEFC powertrain system controlled by a hybrid strategy for rail urban transport, J. Energy Storage 17 (Jun. 2018) 474–484, https://doi.org/10.1016/J.EST.2018.04.011.

[5] K. Jiang, Z. Tian, T. Wen, S. Hillmansen, Y. Zhang, Cost modelling-based route applicability analysis of United Kingdom passenger railway decarbonization options, Int. J. Electr. Power Energy Syst. 160 (Sep. 2024) 110094, https://doi.org/10.1016/J.IJEPES.2024.110094.

[6] M. Kapetanovíckapetanovíc, A. Núñez, N. Van Oort, R.M.P. Goverde, Analysis of hydrogen-powered propulsion system alternatives for diesel-electric regional trains, Journal of Rail Transport Planning & Management 23 (2022) 100338, https://doi.org/10.1016/j.jrtpm.2022.100338.

[7] M. Haji Akhoundzadeh, S. Panchal, E. Samadani, K. Raahemifar, M. Fowler, R. Fraser, Investigation and simulation of electric train utilizing hydrogen fuel cell and lithium-ion battery, Sustain. Energy Technol. Assessments 46 (Aug. 2021) 101234, https://doi.org/10.1016/J.SETA.2021.101234.

[8] J. Lv, J. Kuang, Z. Yu, G. Sun, J. Liu, J.I. Leon, Diagnosis of PEM fuel cell System based on electrochemical impedance spectroscopy and deep learning method, IEEE Trans. Ind. Electron. 71 (1) (Jan. 2024) 657–666, https://doi.org/10.1109/TIE.2023.3241404.

[9] Q. Li, P. Liu, X. Meng, G. Zhang, Y. Ai, W. Chen, Model prediction control-based energy management combining self-trending prediction and subset-searching Algorithm for Hydrogen Electric Multiple unit train, IEEE Transactions on Transportation Electrification 8 (2) (Jun. 2022) 2249–2260, https://doi.org/10.1109/TTE.2022.3149479.

[10] J.P. Torreglosa, P. Garcia, L.M. Fernandez, F. Jurado, Predictive control for the energy management of a fuel-cell-battery- supercapacitor tramway, IEEE Trans. Ind. Inf. 10 (1) (Feb. 2014) 276–285, https://doi.org/10.1109/TII.2013.2245140.

[11] F. Zenith, R. Isaac, A. Hoffrichter, M.S. Thomassen, S. Møller-Holst, Techno-economic analysis of freight railway electrification by overhead line, hydrogen and batteries: case studies in Norway and USA, Proc. Inst. Mech. Eng. F J. Rail Rapid Transit 234 (7) (Aug. 2020) 791–802, https://doi.org/10.1177/0954409719867495.

[12] Roland Berger, Study on the Use of Fuel Cells and Hydrogen in the Railway Environment, 2019.

[13] FNM Group, Museo virtuale ferrovie Nord - Brescia iseo edolo [Online]. Available: https://museo.ferrovienord.it/it/header/stanza-a/brescia-iseo-edolo/. (Accessed 4 October 2024).

[14] Ferrovie Nord Milano, "FNM Group.". https://www.fnmgroup.it/. (Accessed 4 October 2024).

[15] G.V. Lomonossoff, Problems of railway mechanics, Proc. Inst. Mech. Eng. 120 (1) (Jun. 1931) 643–659, https://doi.org/10.1243/PIME_PROC_1931_120_024_02.

[16] S. Lu, S. Hillmansen, C. Roberts, A power-management strategy for multiple-unit railroad vehicles, IEEE Trans. Veh. Technol. 60 (2) (Feb. 2011) 406–420, https://doi.org/10.1109/TVT.2010.2093911.

[17] ALSTOM, Hydrogen Coradia stream description [Online]. Available: www.alstom.com, , 2020.

[18] Y. Ma, C. Li, S. Wang, Multi-objective energy management strategy for fuel cell hybrid electric vehicle based on stochastic model predictive control, ISA Trans. 131 (Dec. 2022) 178–196, https://doi.org/10.1016/J.ISATRA.2022.04.045.

[19] E.D. Kostopoulos, G.C. Spyropoulos, J.K. Kaldellis, Real-world study for the optimal charging of electric vehicles, Energy Rep. 6 (Nov. 2020) 418–426, https://doi.org/10.1016/J.EGYR.2019.12.008.

[20] G. Caramia, N. Cavina, M. Caggiano, S. Patassa, D. Moro, Battery state of charge management strategies for a real-time controller of a Plug-in Hybrid Electric Vehicle, Energy Proc. 148 (Aug. 2018) 258–265, https://doi.org/10.1016/J.EGYPRO.2018.08.076.

[21] G.M. Scheepmaker, R.M.P. Goverde, Energy-efficient train control using nonlinear bounded regenerative braking, Transp. Res. Part C 121 (2020) 102852, https://doi.org/10.1016/j.trc.2020.102852.

[22] K. Ahn, A. Aredah, H.A. Rakha, T. Wei, H.C. Frey, Simple diesel train fuel consumption model for real-time train applications, Energies 16 (8) (2023) 3555, https://doi.org/10.3390/EN16083555, 3555, Apr. 2023.

[23] Rete Ferroviaria Italiana, Aggiornamento Dei Costi Unitari Dell'Energia Relativi Alla Valorizzazione Del Contratto Di Utilizzo 2022/2023, 2023.

[24] H. Gardner, M. Brambilla, and D. Matheus, "Perspectives for the Rolling Stock Supply in the EU Study Policy Department for Structural and Cohesion Policies Directorate-General for Internal Policies PE".

[25] Y. Zhang, Z. Tian, C. Roberts, S. Hillmansen, M. Chen, Cost optimization of multi-mode train conversion for discontinuously electrified routes, Int. J. Electr. Power Energy Syst. 138 (Jun. 2022) 107993, https://doi.org/10.1016/J.IJEPES.2022.107993.

[26] M. Attinà, et al., Written by Assessment of Unit Costs (Standard Prices) of Rail Projects (Capital Expenditure), 2018.

[27] Rete Ferroviaria Italiana, Network statement [Online]. Available: https://www.rfi.it/content/dam/rfi/rfi_en/railway-infrastracture/ns-2025-march-2024/Network_Statement_2025_March%202024.pdf, , 2024. (Accessed 28 June 2024).

[28] M. Raceanu, N. Bizon, M. Varlam, Experimental results for an off-road vehicle powered by a modular fuel cell systems using an innovative startup sequence, Energies 15 (23) (Dec. 2022), https://doi.org/10.3390/en15238922.

[29] R. Stropnik, N. Mlakar, A. Lotrič, M. Sekavčnik, M. Mori, The influence of degradation effects in proton exchange membrane fuel cells on life cycle assessment modelling and environmental impact indicators, Int. J. Hydrogen Energy 47 (57) (Jul. 2022) 24223–24241, https://doi.org/10.1016/J.IJHYDENE.2022.04.011.

[30] Electric and Hybrid Rail Technology - Cummins and Leclanché to collaborate on low emission power solutions for rail. https://www.electricandhybridrail.com/content/news/cummins-and-leclanche-to-collaborate-on-low-emission-power-solutions-for-rail/. (Accessed 29 January 2025).

[31] Alstom - Leclanché. https://www.leclanche.com/clients/alstom/. (Accessed 29 January 2025).

[32] S.A. Lechanché, M3 energy module. https://www.leclanche.com/wp-content/uploads/2021/06/GNMC-65Ah-M3-ENERGY-MODULE.pdf, 2021. (Accessed 20 May 2024).

[33] T. Din, S. Hillmansen, Energy consumption and carbon dioxide emissions analysis for a concept design of a hydrogen hybrid railway vehicle, IET Electr. Syst. Transp. 8 (2) (Jun. 2018) 112–121, https://doi.org/10.1049/IET-EST.2017.0049.

[34] European Hydrogen Observatory, The European hydrogen market landscape. https://observatory.clean-hydrogen.europa.eu/, 2024. (Accessed 18 March 2025).

[35] Deloitte and Ballard, Fueling the Future of Mobility Hydrogen and Fuel Cell Solutions for Transportation -, vol. 1, 2020.

[36] Y. Xie, H. Basma, F. Rodríguez, Purchase costs of zero-emission trucks in the United States to meet future Phase 3 GHG standards [Online]. Available: www.theicct.org, , 2023. (Accessed 8 April 2024).

[37] A.M. Pavan, V. Lughi, M. Scorrano, Total Cost of Ownership of Electric Vehicles Using Energy from a Renewable-based Microgrid, 2019, https://doi.org/10.1109/PTC.2019.8810736.

[38] Q. Cheng, R. Zhang, Z. Shi, J. Lin, Review of Common Hydrogen Storage Tanks and Current Manufacturing Methods for Aluminium Alloy Tank Liners, 2023, https://doi.org/10.1016/j.ijlmm.2023.08.002.

[39] ALSTOM, FNM and Alstom present Italy's first hydrogen-powered train | Alstom [Online]. Available: https://www.alstom.com/press-releases-news/2023/10/fnm-and-alstom-present-italys-first-hydrogen-powered-train. (Accessed 5 September 2024).

[40] E. Fedele, D. Iannuzzi, A. Del Pizzo, Onboard energy storage in rail transport: review of real applications and techno-economic assessments, IET Electr. Syst. Transp. 11 (4) (Dec. 2021) 279–309, https://doi.org/10.1049/ELS2.12026.

[41] F. Brussels, et al., Cost Analysis and high-level Business Case Fuel Cells and Hydrogen Applications for Regions and Cities, 2017.

[42] California Air Resources Board, Draft advanced clean fleets total cost of ownership discussion document [Online]. Available: https://ww2.arb.ca.gov/sites/default/files/2021-08/210909costdoc_ADA.pdf, , 2021. (Accessed 21 June 2024).

[43] ATR catalogue, ATR 125 specifics [Online]. Available: https://spotlog.org/locolist/class/it/ATR+125. (Accessed 5 September 2024).

[44] Agenzia delle Dogane e dei Monopoli, Decreto Legislativo n. 504/95. Art. 24-ter. Punto 4-bis della Tabella A. https://www.adm.gov.it/portale/indirizzi-organigramma-periferico-area-dogane-uffici-dogane, 2023. (Accessed 20 September 2024).

[45] European Union and Prominent, Sustainable, Safe and Economically Feasible Energy Concepts and Technologies for European Inland Shipping D2.8/D2.9 Standardized Model and cost/benefit Assessment for right-size Engines and Hybrid Configurations, 2018.

[46] ABB, Compact Converter BORDLINE® CC750 DE for diesel-electric multiple units. https://search.abb.com/library/Download.aspx?DocumentID=3BHS262330%20ZAB%20E07&LanguageCode=en&DocumentPartId=&Action=Launch. (Accessed 9 May 2024).

[47] FNM Group, H2iseO HYDROGEN VALLEY [Online]. Available: https://www.fnmgroup.it/h2iseo_hydrogen_valley_en/?lang=en. (Accessed 28 June 2024).